

# MULTIPLE RSS FINGERPRINT BASED INDOOR LOCALIZATION IN RIS-ASSISTED 5G WIRELESS COMMUNICATION SYSTEM

Zhaohan Zhang<sup>1</sup>, Liang Wu<sup>1,2</sup>, Zaichen Zhang<sup>1,2</sup>, Jian Dang<sup>1,2</sup>, Bingcheng Zhu<sup>1</sup>, Lei Wang<sup>1</sup>

<sup>1</sup> National Mobile Communications Research Laboratory, Southeast University, Nanjing, 210096, P.R.China

<sup>2</sup> Purple Mountain Laboratory, Nanjing, 211111, P.R.China

Email: {220200882, wuliang, zczhang, dangjian, zbc, wang\_lei\_seu}@seu.edu.cn

Commission IV, WG IV/5

**KEY WORDS:** 5G, CRLB, DNN, indoor localization, multiple RSS fingerprint, PGD.

## ABSTRACT:

The received signal strength (RSS) fingerprint based localization is a widely used technique for location estimation in the indoor environment with the fifth generation (5G) wireless communication. However, the RSS feature is easily affected by the noise and other variations of the propagation channel, thus limiting the localization accuracy. In this paper, we propose a multiple RSS fingerprint based localization scheme in the reconfigurable intelligent surface (RIS) assisted system, where the RSS values under different RIS configurations are leveraged as the fingerprints. However, it is challenging to set the favorable RIS configurations. To tackle this challenge, we design an optimization method based on Cramér-Rao Lower Bound (CRLB) to derive the optimal RIS configurations to achieve a robust and accurate location estimation, where the CRLB is minimized, and projected gradient descent (PGD) method is applied to solve this optimization problem. After the fingerprints are collected, deep neural network (DNN) is employed for location estimation. Simulation results reveal that the proposed scheme performs well in terms of localization accuracy and stability.

## 1. INTRODUCTION

Location information for events, assets, and individuals, mostly focusing on two dimensions so far, has triggered a multitude of applications across different verticals, such as consumer, networking, industrial, health care, public safety, and emergency response use cases. Thus, the localization issue especially the indoor localization has aroused great interest [Zafari et al., 2019].

To enable indoor location based services, various localization techniques have been proposed, among which the fingerprint localization technique based on received signal strength (RSS) in the fifth generation (5G) wireless communication network has gained much attention. Compared with Bluetooth and radio frequency identification (RFID), this 5G-based technique can provide location information with existing 5G base stations (BSs), thus avoiding the cost of deploying any extra equipment. Moreover, different from other fingerprint based techniques, RSS information can be easily collected for its low requirements for hardware.

The RSS-based localization system usually contains two phases, including the offline and the online phases [Wang et al., 2017]. In the first phase, a specific RSS value for each reference point is recorded. And then, the user's location information is estimated by matching the RSS fingerprint in the online phase. However, in the uncontrollable radio environment, the RSS information cannot be customized, and the existence of adjacent locations whose RSS values are similar to each other unavoidably degrades the performance of the localization system.

\* This work is supported by National Key Research and Development Plan (No. 2016YFB0502202), NSFC projects (62171127, 61960206005, 61971136), Research Fund of National Mobile Communications Research Laboratory.

Recently, reconfigurable intelligent surface (RIS) has been proposed as a potential tool to actively change the signal propagation conditions [Zhang et al., 2020]. It is composed of many subwavelength-scale elements with tunable electric response (i.e., phase shifts). By changing the configuration, the RIS is capable of customizing the propagation radio environment in a desired way, and therefore changing the reflected signals. This provides a new way to alter the RSS fingerprint maps and reduce the similarity of the RSS values corresponding to adjacent locations, which can further improve the localization performance.

In this paper, we investigate the problem of fingerprint-based indoor localization in RIS-assisted system for 5G NR network and propose a novel localization scheme which utilizes the multiple RSS values under different RIS configurations as fingerprints. However, such RIS configurations selection is of challenge due to a massive number of possible combinations of phase shifts and the complicated relation between RIS configurations and the RSS fingerprint map. To address this challenge, we first model the channel based on the geometry for Cramér-Rao Lower Bound (CRLB) calculation and then design an optimization method based on CRLB to find the optimal RIS configurations. Besides, the projected gradient descent (PGD) method is utilized to solve this optimization problem. After the fingerprints are collected, deep neural network (DNN) is applied for location estimation. Simulation results show that the proposed scheme performs well and can achieve the localization accuracy of 0.5m in the non-line of sight (NLOS) scenario.

## 2. SYSTEM MODEL

### 2.1 RIS-assisted Indoor Localization Scenario

Consider a typical RIS-assisted wireless communication system, as shown in Fig. 1, which consists of one multiple-antenna

BS, one single-antenna user equipment (UE) and one RIS. The BS receives signals transmitted from the UE in the localization area only through the link reflected by the RIS, while the line-of-sight (LOS) link is blocked due to the existence of the obstacle. We consider a two-dimensional (2D) scenario with uniform linear arrays (ULAs) for both the antenna elements and RIS elements, and the numbers of antenna elements at the BS is  $M$ , while the number of RIS elements is  $N$ .

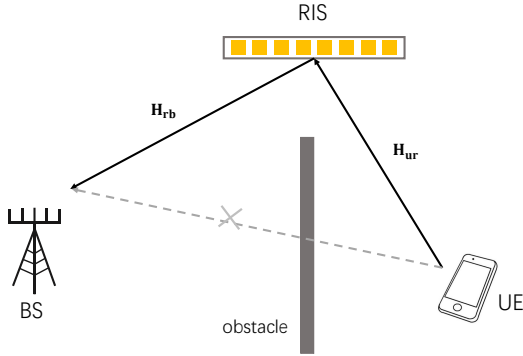


Figure 1. RIS-assisted wireless communication system

Let  $\mathbf{H}$  denote the two tandem channels ( $\mathbf{H}_{ur} \in \mathbb{C}^{N \times 1}$  for the first hop and  $\mathbf{H}_{rb} \in \mathbb{C}^{M \times N}$  for the second hop), which connect the UE to the BS via the RIS. Thus, the entire channel  $\mathbf{H}$  can be formulated as

$$\mathbf{H} = \mathbf{H}_{rb} \mathbf{\Omega} \mathbf{H}_{ur}, \quad (1)$$

where  $\mathbf{\Omega} = \text{diag}(e^{j\omega_1}, e^{j\omega_2}, \dots, e^{j\omega_N}) \in \mathbb{C}^{N \times N}$  is the phase control matrix at the RIS, which is a diagonal matrix with constant-modulus entries in the diagonal. Then, the receive signal can be expressed as

$$\mathbf{Y} = \mathbf{H}\mathbf{X} + \mathbf{W} = (\mathbf{H}_{rb} \mathbf{\Omega} \mathbf{H}_{ur}) \mathbf{X} + \mathbf{W}, \quad (2)$$

where  $\mathbf{X}$  is the transmitted signal and  $\mathbf{W}$  is the noise.

## 2.2 Channel model based on geometric model

In this subsection, the channel is modeled based on the geometry of the considered localization scenario. Assume that the geometry of the localization area is known, then the channel between the UE and the BS can be modeled by the geometry-based channel modeling method (GCM) where Ray-tracing algorithm and the Path Recovery algorithm is applied. The details of GCM is described as follows.

Reflection, diffraction, transmission and scattering will occur when the electromagnetic waves encounter different media. But in general, the signal components except the direct and reflected components are very weak. Therefore, We simplify the receive signal into direct component and reflected component for convenience, where the direct component refers to the signal sent directly from UE to BS, and the reflected component refers to the signal reached BS after several reflections.

Firstly, choose the center point in the localization area as the path reference point (PRP), as shown in Fig 2, then the propagation paths between the PRP and the BS can be obtained by the Ray-tracing algorithm since the locations of all the obstacles is

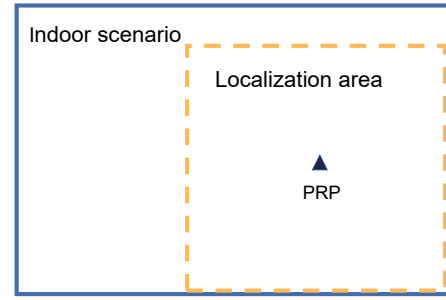


Figure 2. Illustration of PRP

known. It is assumed that the signals transmitted by users in adjacent locations have the same number of propagation paths, and pass by the same reflection surfaces. Therefore, when the localization region is limited, we can recover the paths between the UE in any location and the BS based on the known paths of PRP by employing the path recovery algorithm which leverages the fact that the incident and reflection rays are symmetric with respect to the normal. As shown in Fig. 3, the number of paths  $L$ , the angle of arrival (AOA)  $\mathbf{\Theta} = [\theta_1, \theta_2, \dots, \theta_L]$ , the angle of departure (AOD)  $\mathbf{\Phi} = [\phi_1, \phi_2, \dots, \phi_L]$  and the path length  $\mathbf{\Gamma} = [\gamma_1, \gamma_2, \dots, \gamma_L]$  can be recovered as the output of GCM, and they are expressed as the functions of the UE location  $(x, y)$ . Then, the far-field channel model can be established based on  $L, \mathbf{\Theta}, \mathbf{\Phi}$  and  $\mathbf{\Gamma}$ .

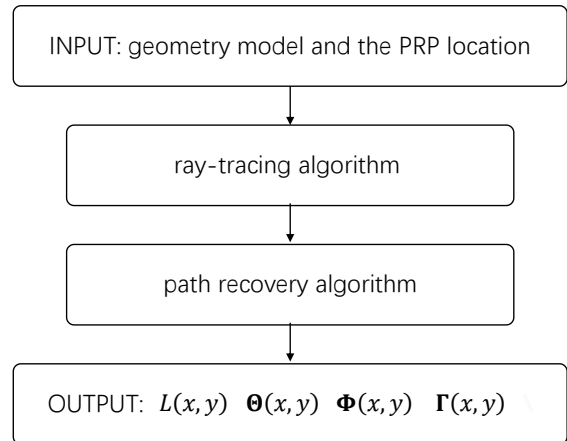


Figure 3. The flow diagram of GCM

Path gain is dependent on the path length and the the number of reflections [Wang and Zhang, 2021]. Assuming that the reflection coefficients of all obstacle surfaces are the same, and the path gain of the  $l^{th}$  path is represented as

$$g(\gamma_l) = \beta^{r_l} \cdot \left( \frac{c}{4\pi f \gamma_l} \right) e^{j2\pi f \gamma_l / c}, \quad (3)$$

where  $\beta$  is the reflection coefficient,  $r_l$  is the number of reflections occurred in the  $l^{th}$  path and  $f$  is the carrier frequency, respectively.

Let  $d$  denote the distance between antennas (or the RIS elements), and  $c$  is the speed of light. If the AOA or AOD is  $\varphi$ , the phase shift between two adjacent antennas (or the RIS elements) caused by the AOA or AOD is  $e^{-j2\pi f d \times \sin(\varphi) / c}$ . There-

fore, the steering vector for both AOA and AOD is given by

$$\boldsymbol{\alpha}(\varphi) = \left[ 1, e^{-j2\pi f d \times \sin(\varphi)/c}, \dots, e^{-j2\pi(M-1) f d \times \sin(\varphi)/c} \right]^T. \quad (4)$$

Let  $L_{ur}$  and  $L_{rb}$  denote the path number of UE-RIS link and RIS-BS link, respectively. Then  $\mathbf{H}_{ur}$  and  $\mathbf{H}_{rb}$  can be modeled as

$$\begin{aligned} \mathbf{H}_{ur} &= \sum_{l=1}^{L_{ur}} g(\gamma_{l,ur}) \boldsymbol{\alpha}(\theta_{l,ur}) \\ \mathbf{H}_{rb} &= \sum_{l=1}^{L_{rb}} g(\gamma_{l,rb}) \boldsymbol{\alpha}(\theta_{l,rb}) \boldsymbol{\alpha}(\phi_{l,rb}), \end{aligned} \quad (5)$$

where  $\theta_{l,rb}$ ,  $\phi_{l,rb}$  and  $\gamma_{l,rb}$  are the AOA, AOD and path length of the  $l^{th}$  path between RIS and BS, respectively, while  $\theta_{l,ur}$  and  $\gamma_{l,ur}$  are the AOA and path length of the  $l^{th}$  path between UE and RIS.

### 2.3 RSS model

During the localization phase, the RSS measured by the BS will be compared with the RSS fingerprints in the database. Let  $\tilde{\mathbf{Y}}_k$  denote the receive signal when RIS is configured as  $\boldsymbol{\Omega}_k$ , then the RSS measured under the configuration  $\boldsymbol{\Omega}_k$  can be expressed as [Zhang et al., 2021]

$$\tilde{s}_k = 10 \lg \left| \tilde{\mathbf{Y}}_k \right|^2. \quad (6)$$

We use the channel response modeled by GCM to calculate the predicted mean RSS, which is only used for the RIS configurations selection. Leveraging the channel model in (5), the predicted mean RSS  $\mu_k$  under the configuration  $\boldsymbol{\Omega}_k$  can be derived as

$$\begin{aligned} \mu_k &= 10 \lg \left| (\mathbf{H}_{rb} \boldsymbol{\Omega}_k \mathbf{H}_{ur}) \mathbf{X} \right|^2 \\ &= 10 \lg \left| \left( \sum_{l=1}^{L_{rb}} g(\gamma_{l,rb}) \boldsymbol{\alpha}(\theta_{l,rb}) \boldsymbol{\alpha}(\phi_{l,rb}) \right. \right. \\ &\quad \left. \left. \times \boldsymbol{\Omega}_k \sum_{l=1}^{L_{ur}} g(\gamma_{l,ur}) \boldsymbol{\alpha}(\theta_{l,ur}) \right) \mathbf{X} \right|^2. \end{aligned} \quad (7)$$

## 3. THE PROPOSED SCHEME

### 3.1 System architecture

In this paper, we aim to improve the localization accuracy by developing a RSS fingerprint based indoor localization system which utilizes the RIS to create multiple RSS fingerprints. The overall localization system architecture is shown in Fig. 4, which can be divided into two phases, including the RIS configuration selection phase and localization phase.

**3.1.1 RIS configuration selection phase** In the proposed RIS based localization scheme, the RSS values under different RIS configurations are selected as the fingerprints. The RIS has the potential to change the signal propagation conditions, and the phase shift of each elements in the RIS is alterable. By adjusting the RIS configuration, the RSS in BS will be changed

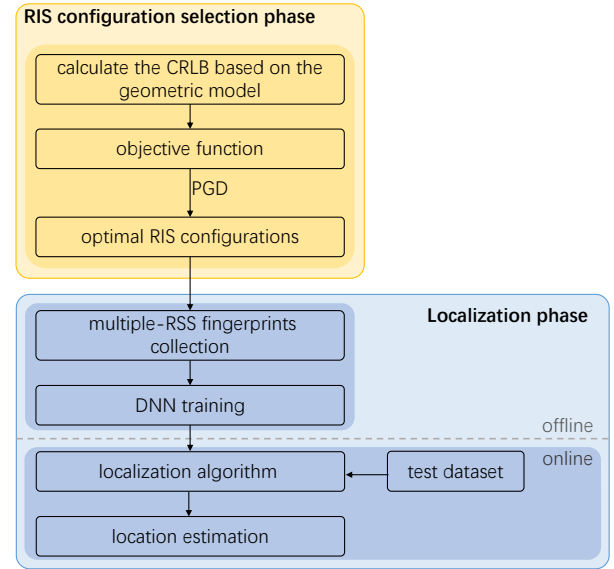


Figure 4. Localization architecture of the proposed localization scheme

significantly, and a sequence of RSS signatures under different phase shifts can be created for each location.

However, it is challenging to set the phase shift of each element for a higher localization accuracy. Therefore, we design an optimization method based on CRLB to find the favorable RIS configurations to achieve a robust and accurate location estimation. The optimal RIS configurations are selected by minimizing the CRLB in the PRP, and projected gradient descent (PGD) method is applied to solve the optimization problem. After determining the optimal RIS configurations, the multiple RSS values under the optimal RIS configurations can be recorded as fingerprints and stored in the training database.

**3.1.2 Localization Phase** The localization phase can further be divided into two stages, including the offline training stage and online positioning stage. The main work in the offline stage is to train the machine learning framework based on the training database. In the online stage, the measured multiple RSS values are used to estimate the location of the test points.

In this phase, we employ a DNN regression algorithm to extract features based on the fingerprint database. After training, the RSS values under the preset RIS configurations of the unknown location is fed into the trained DNN, which outputs the estimated location coordinate.

### 3.2 CRLB

In this subsection, the expression of the CRLB for the multiple RSS based localization is derived. Suppose that the RSS values under  $K$  different RIS configurations are selected as fingerprint features, and let the set  $\{\boldsymbol{\Omega}_1, \boldsymbol{\Omega}_2, \dots, \boldsymbol{\Omega}_K\}$  denote the  $K$  configuration matrices. The distribution of RSS under the RIS configuration  $\boldsymbol{\Omega}_k$  can be approximated by the Gaussian distribution. Assuming that the UE locates in  $\mathbf{P} = [x, y]$ , the joint probability density of the  $K$  RSS values under different RIS configurations can be expressed as

$$p(S; \mathbf{P}) = \prod_{k=1}^K \frac{1}{\sqrt{2\pi}\sigma} \exp \left[ -\frac{s_k - \mu_k(\mathbf{P})}{2\sigma^2} \right], \quad (8)$$

where  $\mathbf{S} = [s_1, s_2, \dots, s_K]$  is the observed RSS matrix,  $\sigma$  is the standard deviation and  $\mu_k(\mathbf{P})$  is the predicted mean RSS which is presented in (7).

The lower bound is given in terms of the Fisher Information Matrix (FIM) [Werner et al., 2016]. If  $p(s; \mathbf{P})$  denotes the probability density function (p.d.f.) of observations  $s$  conditioned on  $\mathbf{P}$ , the score function is defined as the gradient of its log-likelihood, that is,

$$\mathbf{U}(\mathbf{P}) = \nabla \ln p(s; \mathbf{P}) = \frac{\partial}{\partial \mathbf{P}} \ln p(s; \mathbf{P}). \quad (9)$$

The FIM  $J(P)$  is the variance of this score function, and can be expressed as

$$\mathbf{J}(\mathbf{P}) = \mathbb{E} \left\{ \left[ \frac{\partial \ln p(s; \mathbf{P})}{\partial \mathbf{P}} \right]^2 \right\}. \quad (10)$$

If  $p(s; P)$  belongs to the exponential family, it can be derived as

$$\mathbf{J}(\mathbf{P}) = -\mathbb{E} \left\{ \frac{\partial \mathbf{U}(\mathbf{P})}{\partial \mathbf{P}} \right\}. \quad (11)$$

The CRLB is the inverse of FIM and can be calculated as

$$\text{Cov}_\theta(\hat{\theta}) \geq \{J(\theta)\}^{-1}. \quad (12)$$

The FIM is given by,

$$\mathbf{J}(\mathbf{P}) = \begin{bmatrix} J_{xx}(\mathbf{P}) & J_{xy}(\mathbf{P}) \\ J_{yx}(\mathbf{P}) & J_{yy}(\mathbf{P}) \end{bmatrix}, \quad (13)$$

where

$$\begin{aligned} J_{xx} &= \frac{1}{\sigma^2} \sum_{k=1}^K \left( \frac{\partial \mu_k}{\partial x} \right)^2 \\ J_{yy} &= \frac{1}{\sigma^2} \sum_{k=1}^K \left( \frac{\partial \mu_k}{\partial y} \right)^2 \\ J_{xy} = J_{yx} &= \frac{1}{\sigma^2} \sum_{k=1}^K \left( \frac{\partial \mu_k}{\partial x} \cdot \frac{\partial \mu_k}{\partial y} \right). \end{aligned} \quad (14)$$

If  $\text{Var}(\hat{P})_K$  denotes the variance of the location estimation, from the CRLB property, we have,

$$\text{Var}(\hat{\mathbf{P}})_K \geq \frac{J_{xx} + J_{yy}}{|J(x, y)|}, \quad (15)$$

where  $|J(x, y)| = J_{xx} \cdot J_{yy} - J_{xy} \cdot J_{yx}$ . Then, the CRLB can be expressed as

$$C_K = \sigma^2 \frac{\sum_{k=1}^K \left( \frac{\partial \mu_k}{\partial x} \right)^2 + \sum_{k=1}^K \left( \frac{\partial \mu_k}{\partial y} \right)^2}{\left[ \sum_{k=1}^K \left( \frac{\partial \mu_k}{\partial x} \right)^2 \right] \cdot \left[ \sum_{k=1}^K \left( \frac{\partial \mu_k}{\partial y} \right)^2 \right] - \left[ \sum_{k=1}^K \left( \frac{\partial \mu_k}{\partial x} \cdot \frac{\partial \mu_k}{\partial y} \right) \right]^2}. \quad (16)$$

### 3.3 RIS Configuration Settings

In this paper, we aim to optimize the RIS configurations by minimizing the CRLB in the PRP. To describe the optimization al-

gorithm, we firstly define the following set as

$$\Psi = \left\{ \mathbf{T} \in \mathbb{R}^{N \times N} \mid 0 \leq t_{i,j} < 2\pi, i, j = 1, 2, \dots, N \right\}. \quad (17)$$

Let  $(x_p, y_p)$  denote the location of the PRP. Accordingly, the optimization problem can be formulated as

$$\begin{aligned} &\underset{\Omega_k}{\text{minimize}} && F(\Omega_1, \Omega_2, \dots, \Omega_K) = C_K(x_p, y_p) \\ &\text{subject to} && \Omega_k \in \Psi \quad (k = 1, 2, \dots, K), \end{aligned} \quad (18)$$

where  $\Omega_k = \text{diag}(e^{j\omega_{k,1}}, e^{j\omega_{k,2}}, \dots, e^{j\omega_{k,N}})$  is the  $k^{\text{th}}$  RIS phase control matrix and  $\omega_{k,n}$  is the phase shift of the  $n^{\text{th}}$  RIS element in  $\Omega_k$ .

Then we use PGD for optimization [Perovi et al., 2021]. It is clear that  $\Psi$  is the feasible set of (15). Let  $\Xi_\Psi(\mathbf{b})$  denote the projection from a matrix  $\mathbf{b}$  onto the set  $\Psi$ .

---

#### Algorithm 1 Projected Gradient Descent Method

---

**Input:**  $\varepsilon$

**Output:**  $\Omega_{1,opt}, \Omega_{2,opt}, \dots, \Omega_{K,opt}$

1: Objective Function:  $F(\Omega_1, \Omega_2, \dots, \Omega_K) = C_K(x_p, y_p)$

2: Initialization: set  $\Omega_{1,0}, \Omega_{2,0}, \dots, \Omega_{K,0}$

3:  $i = 1$

4: **repeat**

5:   calculate the gradient  $\nabla F$  as the iteration direction

6:   update the step length  $\lambda_i$  by linear search

7:    $\Omega_{k,i} = \Omega_{k,i-1} - \lambda_i \cdot \frac{\partial F}{\partial \Omega_{k,i-1}}, k = 1, 2, \dots, K$

8:    $\Omega_{k,i} = \Xi_\Psi(\Omega_{k,i}), k = 1, 2, \dots, K$

9:    $i = i + 1$

10: **until**  $\|\nabla F(\Omega_{1,i-1}, \Omega_{2,i-1}, \dots, \Omega_{K,i-1})\| < \varepsilon$

---

The optimization algorithm is provided in Algorithm 1 and the main idea behind PGD is as follows. Firstly, start from the arbitrary initial values  $\Omega_{1,0}, \Omega_{2,0}, \dots, \Omega_{K,0}$ . The parameter  $\Omega_k$  is changed in each iteration in the direction of the gradient  $\nabla F(\Omega_1, \Omega_2, \dots, \Omega_K)$ . The size of this move is determined by the step size  $\lambda_i$  which is set by linear search method. As a result of this step, the resulting updated configuration matrices may lie outside of the feasible set. Therefore, before the next iteration, we project the newly computed matrices  $\Omega_{k,i}$ , ( $k = 1, 2, \dots, K$ ), onto  $\Psi$ , respectively. The iteration stops when the objective function converges. The objective function is said to converge when  $\|\nabla F\| < \varepsilon$ , where  $\varepsilon$  is the convergence bound.

### 3.4 Localization Phase

In the training stage, the fingerprints are recorded at each sampling location in the area of interest. We use the  $K$  RSS values under the selected optimal RIS configurations as fingerprints. Let  $\tilde{\mathbf{S}} = [\tilde{s}_1, \tilde{s}_2, \dots, \tilde{s}_K]$  denote the set of these  $K$  measured RSS values, and the form of the fingerprint at each point is shown in TABLE I.

Table 1. Form of the multiple RSS fingerprint database

feature			label	
$\tilde{s}_1$	$\tilde{s}_2$	$\dots$	$\tilde{s}_K$	$x$
				$y$

The DNN is then trained based on the fingerprints of all the sampling locations labeled with their coordinates. We train the DNN model to determine the structure of this network and the weights and biases of the neurons. The final DNN model is presented in Fig. 5.

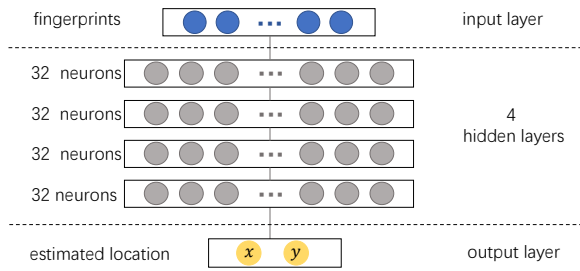


Figure 5. Structure of DNN

1. Structure of DNN: We employ a fully connected DNN to fulfill the task of localization with beam amplitude fingerprints. The DNN model has 4 fully connected hidden layers, plus one input layer, and one output layer. Each hidden layer has 32 neurons. The input to the DNN model is the fingerprints, and the output of the DNN model is location coordinate  $(x, y)$ .
2. Activation Function: The activation function introduces nonlinearity into DNN and is an important factor in performance. We choose Rectified Linear Units (ReLU) as the activation function, which is expressed as

$$\text{ReLU}(x) = \max(0, x) \quad (19)$$

3. Loss Function: We use the error loss function based on back propagation to train the weights and biases of the neurons. The loss function is employed to measure the difference between the ground truth and the output of the DNN model, which we define as the mean distance error

$$f_{\text{loss}} = \frac{1}{\kappa} \sum_{i=1}^{\kappa} \sqrt{(\hat{x}_i - x_i)^2 + (\hat{y}_i - y_i)^2} \quad (20)$$

where  $\kappa$  is the batch size,  $(x_i, y_i)$  and  $(\hat{x}_i, \hat{y}_i)$  represent the true and the estimated coordinates of sample  $i$ , respectively. By minimizing the value of  $f_{\text{loss}}$ , the neuron weights and biases are updated with adaptive moment estimation (Adam) algorithm, until the value of  $f_{\text{loss}}$  converges.

During training, the multiple RSS fingerprints of all the reference points are fed into the DNN in batches to train the weights and biases of the neurons. Then, weights and biases are stored as constants of the DNN model for online stage. During localization, the CSI fingerprints of the target point is fed into the trained DNN, which outputs the location coordinate  $(x, y)$ .

#### 4. SIMULATION RESULTS

Simulation is performed in the test site with size  $50m^2$ . As shown in Fig. 6, the BS is equipped at  $(0m, 3m)$ , and the RIS is equipped at  $(5m, 5m)$ . The area of interest is a  $3m \times 3m$  workshop, which is marked in the blue dotted box. All the obstacle surfaces in this scene are assumed to be smooth reflective surfaces with the same reflection coefficient  $\beta = 0.8$ . The BS is equipped with 4 antennas ( $M = 4$ ) and the RIS consists of 6 elements ( $N = 6$ ), and both of them are arranged in ULA. We use 5G New Radio (NR) signals generating according to the 3GPP standards as transmit signals.

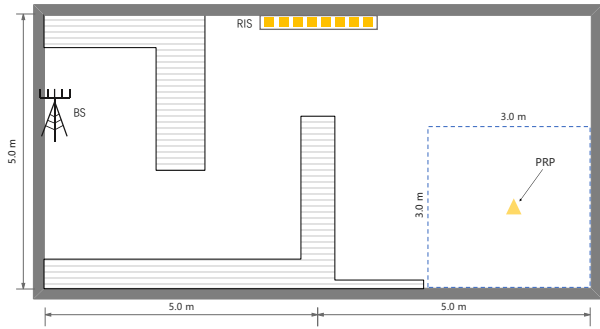


Figure 6. Layout of the simulation

We first provide the effectiveness of the optimization algorithm. It can be observed from Fig. 7 that the CRLB of the PRP decreases quickly, and can get convergence after several iterations. The convergence value with  $K = 3$  is less than the case with  $K = 2$ , consistent with the fact that the increase of fingerprint dimension can improve the localization performance, which is shown in Fig. 8. In addition, it is noted that the value of the objective function can attain about 0.11 with  $K = 3$  and SNR = 30dB.

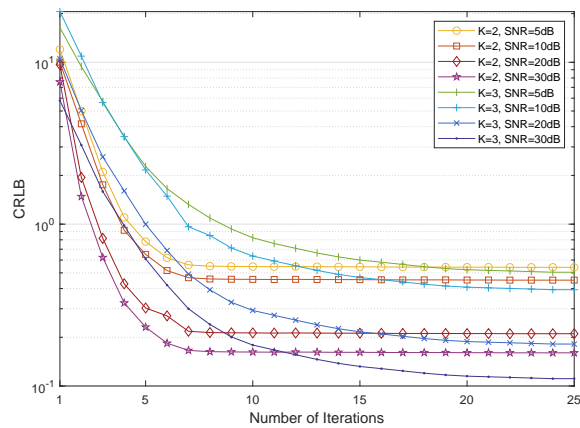


Figure 7. The convergence behaviour of the PGD algorithm

To evaluate the performance of the proposed localization scheme, we give the performance obtained by three schemes: the conventional RSS scheme without RIS, the multiple-RSS scheme with random RIS configurations, and the multiple-RSS scheme with the optimal RIS configurations. In the conventional RSS scheme, the RSS without RIS is used as fingerprint and the localization error is about 0.61m in this scenario when SNR=10dB. In the scheme with random RIS configurations, the mean localization error is about 0.55m when  $K = 3$  and 0.57m when  $K = 2$ . Our scheme based on the optimal RIS configurations decided by PGD significantly outperforms the first two schemes and the mean localization error can reach 0.46m with  $K = 3$  and SNR=10dB. Moreover, when SNR increases, the positioning performance of our proposed scheme will also become better. Particularly, the localization error can reach 0.16m when  $k = 3$  and SNR = 10dB.

#### 5. CONCLUSION

In this paper, an intelligent RIS-assisted localization scheme is proposed, which is based on the multiple RSS fingerprints and

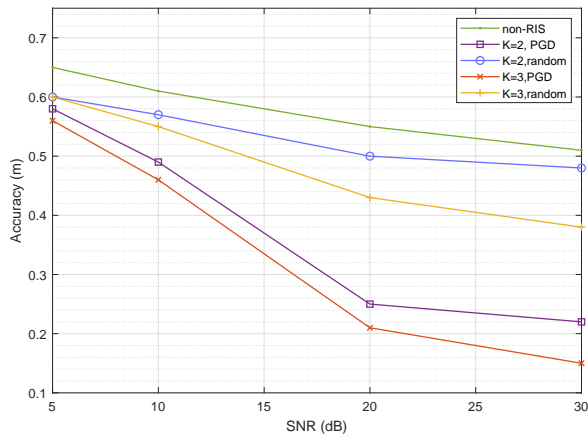


Figure 8. Localization performance

DNN. We use the multiple RSS values under different RIS configurations as fingerprints, and design an optimization method based on CRLB to find the optimal RIS configurations. Besides, DNN regression network is trained for localization. The performance of the localization method is evaluated in certain scenario. Simulation results show that the proposed scheme is able to achieve a robust and accurate location estimation, which is about 0.5m in the NLOS scenario. The proposed localization scheme is a strong candidate for the 5G and future wireless communication systems.

## REFERENCES

- Perovi, N. S., Tran, L.-N., Di Renzo, M., Flanagan, M. F., 2021. Achievable Rate Optimization for MIMO Systems With Reconfigurable Intelligent Surfaces. *IEEE Transactions on Wireless Communications*, 20(6), 3865-3882.
- Wang, W., Zhang, W., 2021. Joint Beam Training and Positioning for Intelligent Reflecting Surfaces Assisted Millimeter Wave Communications. *IEEE Transactions on Wireless Communications*, 20(10), 6282-6297.
- Wang, X., Gao, L., Mao, S., 2017. BiLoc: Bi-Modal Deep Learning for Indoor Localization With Commodity 5GHz WiFi. *IEEE Access*, 5, 4209-4220.
- Werner, J., Wang, J., Hakkarainen, A., Cabric, D., Valkama, M., 2016. Performance and CramerRao Bounds for DoA/RSS Estimation and Transmitter Localization Using Sectorized Antennas. *IEEE Transactions on Vehicular Technology*, 65(5), 3255-3270.
- Zafari, F., Gkelias, A., Leung, K. K., 2019. A Survey of Indoor Localization Systems and Technologies. *IEEE Communications Surveys Tutorials*, 21(3), 2568-2599.
- Zhang, H., Hu, J., Zhang, H., Di, B., Bian, K., Han, Z., Song, L., 2020. MetaRadar: Indoor Localization by Reconfigurable Metamaterials. *IEEE Transactions on Mobile Computing*, 1-1.
- Zhang, H., Zhang, H., Di, B., Bian, K., Han, Z., Xu, C., Zhang, D., Song, L., 2021. Rss fingerprinting based multi-user outdoor localization using reconfigurable intelligent surfaces. *2021 15th International Symposium on Medical Information and Communication Technology (ISMICT)*, 167-172.